Cell Death and Differentiation (2014) 21, 696–706

www.nature.com/cdd

Caspase-6 activity in the CA1 region of the hippocampus induces age-dependent memory impairment

AC LeBlanc*[,1,2], J Ramcharitar[1,2], V Afonso[1,2], E Hamel[2,3], DA Bennett[4,5], P Pakavathkumar[1,2] and S Albrecht[6]

Active Caspase-6 is abundant in the neuropil threads, neuritic plaques and neurofibrillary tangles of Alzheimer disease brains. However, its contribution to the pathophysiology of Alzheimer disease is unclear. Here, we show that higher levels of Caspase-6 activity in the CA1 region of aged human hippocampi correlate with lower cognitive performance. To determine whether Caspase-6 activity, in the absence of plaques and tangles, is sufficient to cause memory deficits, we generated a transgenic knock-in mouse that expresses a self-activated form of human Caspase-6 in the CA1. This Caspase-6 mouse develops age-dependent spatial and episodic memory impairment. Caspase-6 induces neuronal degeneration and inflammation. We conclude that Caspase-6 activation in mouse CA1 neurons is sufficient to induce neuronal degeneration and age-dependent memory impairment. These results indicate that Caspase-6 activity in CA1 could be responsible for the lower cognitive performance of aged humans. Consequently, preventing or inhibiting Caspase-6 activity in the aged may provide an efficient novel therapeutic approach against Alzheimer disease.
Cell Death and Differentiation (2014) **21,** 696–706; doi:10.1038/cdd.2013.194; published online 10 January 2014

The underlying molecular pathway for neuronal degeneration and dysfunction in Alzheimer's disease (AD) remains unknown. Yet, the identification of critical events initiating neuronal degeneration could provide a novel therapeutic approach to stem the progressive dementia of AD. We propose that Caspase-6 (Casp6), a cysteinyl protease of the caspase family, has a critical role in AD neuronal degeneration and cognitive impairment. Casp6 activity is intimately associated with the neuritic plaques (NP), neurofibrillary tangles (NFT), and neuropil threads (NPT) of AD.[1] Casp6 activity is abundant in familial AD[2] and at all stages of sporadic AD.[3] Although no Casp6 activity is present in younger brains,[1] several aged non-cognitively impaired (NCI) brains show significant amounts of Casp6 activity in the entorhinal cortex (ERC),[3] the first area showing NFT pathology in AD according to Braak staging.[4,5] Furthermore, higher levels of Casp6 activity in the ERC and cornu ammonis 1 (CA1) region of NCI brains correlate with lower episodic memory (EP) performance, one of the types of memory also affected early in AD.[6]

Active Casp6 induces several parallel degenerative pathways associated with AD neuropathology. First, Casp6 activity disrupts the neuronal cytoskeleton. Casp6 cleaves neuronal microtubule protein alpha-tubulin, microtubule-associated protein Tau, and actin-regulating post-synaptic density proteins, Spinophilin, Drebrin, and Actinins.[7] In mouse, caspase activity precedes and leads to the formation of NFT-like aggregation.[8] Casp6 activity is involved in axonal degeneration of mouse PNS neurons via amyloid precursor protein (APP) interaction with death receptor 6[9] and in nerve growth factor (NGF)-deprived dorsal root ganglion neurons.[10] Furthermore, Casp6-dependent axonal degeneration is modulated by NGF deprivation of the axonal compartment.[11] Casp6-mediated neurodegeneration also occurs in myelin- and p75NTR (neurotrophin factor)-dependent axonal degeneration in adult mouse brains.[12,13] In human primary neurons, overexpression of wild-type (WT) or mutant APP induces Casp6-dependent, but amyloid beta peptide (Aβ)-independent, axonal degeneration.[14] Second, Casp6 activity in primary human neurons increases the production of Aβ.[15,16]

[1]Bloomfield Center for Research in Aging, Lady Davis Institute for Medical Research, Jewish General Hospital, 3755 Ch. Cote Ste-Catherine, Montreal, QC H3T 1E2, Canada; [2]Department of Neurology and Neurosurgery, McGill University, 3775 University St., Montreal, QC H3A 2B4, Canada; [3]Montreal Neurological Institute, 3801 rue University, Montreal, QC H3A 2T5, Canada; [4]Rush Alzheimer's Disease Center, Rush University Medical Center, 600S. Paulina, Suite 1028, Chicago, IL, USA; [5]Department of Neurological Sciences, Rush University Medical Center, 1725 West Harrison, Chicago, IL, USA and [6]Department of Pathology, McGill University, and Montreal Children's Hospital, Montreal, QC H3A 2B4, Canada

*Corresponding author: AC LeBlanc, Bloomfield Center for Research in Aging, Lady Davis Institute for Medical Research, Sir Mortimer B Davis Jewish General Hospital, 3755 Ch. Côte Ste-Catherine, Montréal, QC H3T 1E2, Canada. Tel: +1 514 340 8260; Fax: +1 514 340 8295; E-mail: andrea.leblanc@mcgill.ca

Keywords: Alzheimer disease; Caspase-6; cognitive impairment; aging; neurodegeneration

Abbreviations: Aβ, amyloid beta peptide; AD, Alzheimer's disease; APP, amyloid precursor protein; ARC, arcuate nucleus; CA1 or CA2, cornu ammonis 1 or 2; CaMKIIa, calmodulin kinase IIa; Casp, caspase; CHAPS, 3-[(3-cholamidopropyl) dimethylammonio]-1-propanesulfonate; CLB, cell lysis buffer; Cre, Cre recombinase; EP, episodic memory; ERC, entorhinal cortex; GFAP, glial fibrillary acidic protein; GGA3, Golgi-associated, gamma adaptin ear containing, ARF-binding protein 3; hCasp6, human Caspase-6; HPRT, hypoxanthine-guanine phosphoribosyl transferase; KI, knock-in; MCI, mild cognitive impairment; MMSE, mini mental state exam; NCI, non-cognitive impairment; NGF, nerve growth factor; NFT, neurofibrillary tangles; NOR, novel object recognition; NP, neuritic plaques; NPT, neuropil threads; PAGE, polyacrylamide gel electrophoresis; PS, perceptual speed; RIPA, radioimmunoprecipitation assay; SE, semantic memory; SO, stratum oriens; SLM, stratum lacunosum molecular; SR, stratum radiatum; VSA, visuospatial ability; WO, working memory; WT, wild type

Received 13.6.13; revised 29.11.13; accepted 03.12.13; Edited by P Bouillet; published online 10.1.14

Although APP is a substrate of Casp6,[16–18] the caspase-dependent increase of Aβ is due to the cleavage of GGA3 (Golgi-associated, gamma adaptin ear containing, ARF-binding protein 3), an inhibitor of beta secretase.[19,20] Third, Casp6 cleaves valosin-containing protein resulting in the accumulation of cytosolic ubiquitinated misfolded proteins through an impairment of the ubiquitin–proteasomal system.[21] Therefore, Casp6 activation in neurons affects several neuronal structures and pathways that are essential to neuronal function.

Together, these studies show an association of Casp6 with several of AD neuropathological lesions. Unlike the other effector caspases, Casp3 and Casp7, active Casp6 does not directly induce apoptotic cell death.[1,22,23] However, in many cell types, Casp6 can activate Casp3-mediated apoptosis[24–26] and Casp3 can activate Casp6.[27] Casp6 cleaves Lamin A and is responsible for chromatin condensation in apoptotic cells.[28–31] Despite significant evidence supporting the role of active Casp6 in AD-related pathologies and cognitive impairment, there is no direct evidence that Casp6 can induce neuronal dysfunction in AD in the absence of NP and NFT. Here, we show that higher Casp6 activity in the CA1 region of NCI aged individuals correlates with lower performance in declarative memory, which is among the earliest clinical symptom of AD.[32] We directly address the role of Casp6 activity in the hippocampus by overexpressing a self-activated form of human Casp6 (hCasp6) in the mouse CA1. We find that Casp6 activation in the mouse CA1 induces neuronal degeneration and age-dependent spatial and EP impairment.

Results

Casp6 activity in CA1 neurons of aged NCI individuals is associated with lower declarative memory performance. Casp6 activity is detected in the NFT, NP, and NPT of human brains with antisera against the active p20 subunit of Casp6 and Tau protein cleaved by Casp6 (TauΔCasp6) (Figure 1a). The antisera did not immunostain pathology-free cerebellum AD tissue and some aged non-AD (NCI) brain tissues, and the adsorption of the antisera on their respective recombinant proteins eliminated immunostaining on AD tissues (Supplementary Figure S1). In AD, Casp6 activity was abundantly present in all the affected brain regions, even in the mild forms of AD (Figure 1b).[3] Surprisingly, some NCI aged individuals cognitively ascertained within a year of death showed abundant Casp6 activity in NFT and NPT in layers II and III of the ERC (Figure 1c). In some aged NCI cases, Casp6 activity was observed in the subiculum but not in the CA1 region (Figure 1c), while in other cases Casp6 activity occurred in the CA1 region, as observed in AD (Figure 1b), albeit at a much lower level. Previously, a semi-quantitative assessment correlated the amount of Casp6 activity in ERC and CA1 with lower performance in declarative memory.[6] The Casp6 activity measured with neoepitope anti-active Casp6 immunostaining correlated significantly with neoepitope TauΔCasp6 immunostaining, and each immunostaining correlated similarly with a lower performance in cognitive abilities in the CA1 region of the hippocampus. Herein, a more in-depth quantitative analysis of the amount of TauΔCasp6/mm^2 in the CA1 of 16 aged NCI cases (demographics and cognitive scores are in Table 1) showed that the level of Casp6 activity assessed with TauΔCasp6 immunohistological staining correlated negatively with global cognitive scores (Spearman rank $r=-0.615$, $P=0.011$) and declarative EP ($r=-0.639$; $P=0.008$) and semantic memories (SEs: $r=-0.562$, $P=0.023$) (Figure 1d). In contrast, no correlations were obtained with working memory (WO), perceptual speed (PS), or visuospatial ability (VSA) scores, three cognitive abilities affected later in AD. The levels of Casp6 activity also did not correlate with the mini mental state exam (MMSE), Braak stage (Figure 1d), age ($r=0.438$, $P=0.090$), education ($r=0.354$, $P=0.179$), and post-mortem intervals ($r=-0.279$, $P=0.493$). Together, these results indicate that Casp6 activity in the hippocampal CA1 region associates with lower declarative cognitive performance in aged individuals and may presage the onset of AD.

Generating a mouse model of Casp6 overexpression in the hippocampus. To assess whether activation of Casp6 in the CA1 is responsible for the lower cognitive performance of NCI individuals, we generated a transgenic mouse expressing a self-activating form of hCasp6 in the CA1 region of the hippocampus (knock-in (KI)/Cre (Cre recombinase)) (Figure 2a). Excision of the STOP sequence of the KI transgene by Cre (Figure 2b) and expression of human p20p10Casp6 was confirmed by RT-PCR (Figure 2c) and western blotting analyses (Figure 2d). Consistent with reports that the T29.1 calmodulin kinase IIa (CaMKIIa)-Cre on C57Bl/6 background express Cre almost exclusively in the CA1 pyramidal neurons of the hippocampus 2–3 weeks after birth,[33] hCasp6 expression was detected with a hCasp6-specific antibody in the CA1 region of the Casp6 KI/Cre mouse brains between 2 and 24 months of age (Figure 2e, controls for antibody in Supplementary Figure S2). The relative sparcity of Casp6 in the neuronal pyramidal cell layer (PCL) (2–3 per CA1 in each 4-μm tissue section) and the presence of Casp6 in axons and dendrites of the stratum oriens (SO), stratum radiatum (SR), and stratum lacunosum moleculare (SLM) of the CA1 region (Figure 2f) is consistent with the expected localization of active Casp6 in neurites.[9] Expression of hCasp6 in the KI/Cre mice was detected in CA1 and occasionally in the CA2 (6% of cases; Figure 2g). The expression of hCasp6 was slightly leaky in the KI/WT as hCasp6 immunoreactivity was detected in the CA1 of 14.3% of cases and in the CA2 of 7.1% of cases. As expected, there was no hCasp6 immunoreactivity in WT/Cre mice CA1 or CA2 regions and in the acuate nucleus (ARC) of either the KI/Cre, KI/WT, or WT/Cre. Western blots against tubulin cleaved by Casp6 (TubulinΔCasp6)[7] confirmed the activity of Casp6 in the hippocampus, but not in the cerebellum, of the KI/Cre mice or in the KI/WT and WT/Cre mice hippocampi or cerebellum (Figure 2h). TubulinΔCasp6 was detected in the CA1 PCL neurons of the KI/Cre and in punctate structures in the SO, SR, and SLM (Figure 2i), a pattern of immunoreactivity that closely mimicked that observed with anti-hCasp6. In contrast, no TubulinΔCasp6 immunoreactivity was observed in these regions in WT/Cre and Casp6 null brains (Figure 2i). Immunoreactivity against

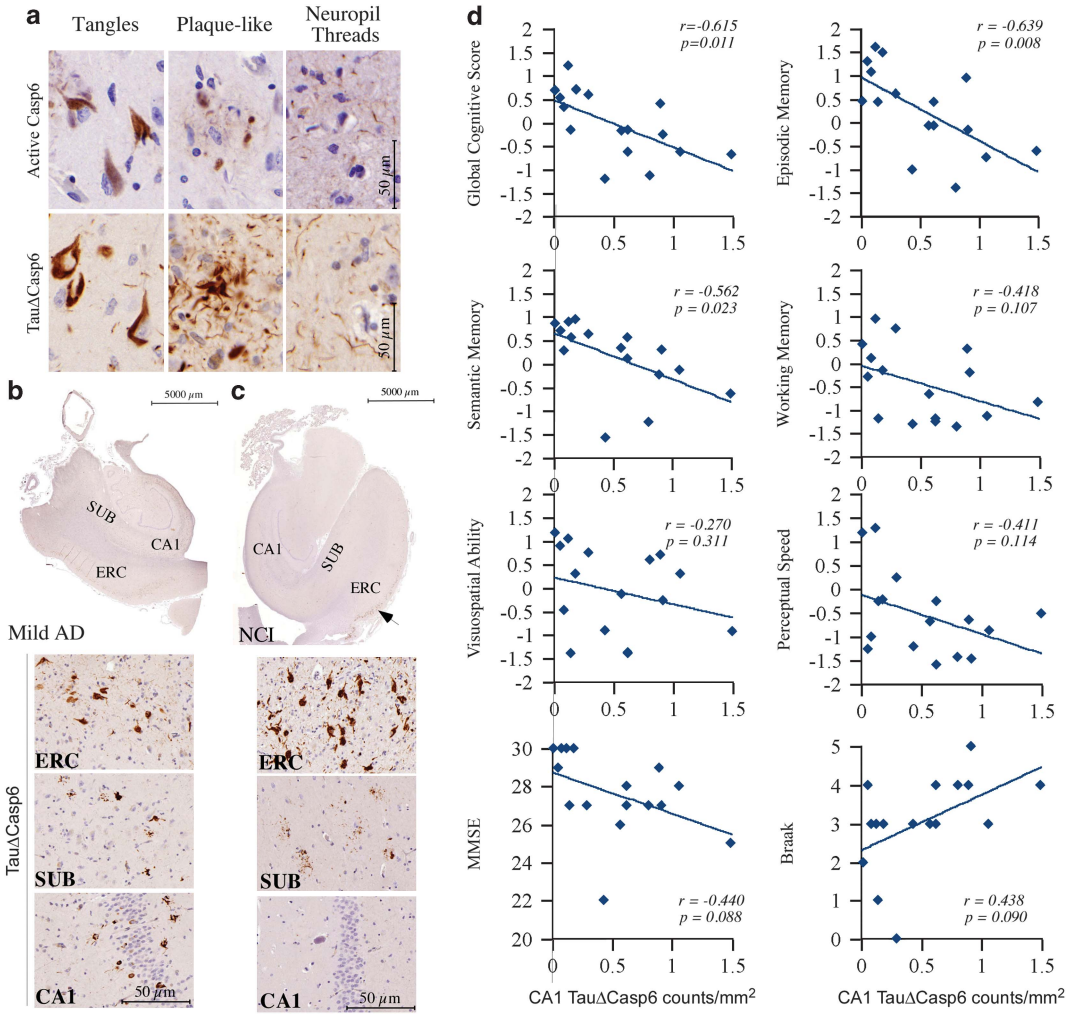

Figure 1 Casp6 activity in human hippocampal CA1 correlates with lower cognitive performance in aged individuals. (**a**) Micrographs of AD brain tissue sections showing positive immunostaining of NFT, NP, and NPT with anti-active Casp6 and anti-TauΔCasp6. The specificity of the neoepitope antisera is shown in Supplementary Figure S1. (**b** and **c**) Immunohistochemistry of TauΔCasp6 in mild AD (**b**) and NCI (**c**) entorhinal cortex (ERC), subiculum (SUB), and CA1. (**d**) Correlation between the level of TauΔCasp6 in the CA1 and performance of various memory tests and Braak staging. *r* indicates Pearson rank correlation value and statistical significance was established by a two-tail *P*-value

TubulinΔCasp6 appeared at 9 months of age and was found most abundantly in the oldest mouse brains tested (24 months). Furthermore, an antibody against active Casp6 immunostained the CA1 neuronal cytoplasm and neurites of the KI/Cre mice hippocampus specifically (Figure 2j). No immunopositivity was detected in other areas of the KI/Cre brain and in the brains, including the hippocampus, of the KI/WT and WT/Cre. Together, these results show that we have generated a mouse expressing active Casp6 in the hippocampal CA1.

Casp6 overexpression in mouse CA1 results in age-dependent memory impairment. Assessing spatial memory with a Morris water maze revealed that the KI/Cre mice expressing hCasp6 in the CA1 of the hippocampus undergo age-dependent memory decline. Initially (Days 1–3), the mice were submitted to a visual platform task to assess their ability to reach the platform within 30 s (stimulus–response learning). Adult (<15 months; Supplementary Figure 3SA) and old (≥15 months; Supplementary Figure 3SB) KI/Cre, KI/WT, or WT/Cre mice performed similarly. Likewise, in the hidden platform task (spatial reference memory) the three groups of adult and old mice did not show significant differences in performance at any age (Days 4–8 in Supplementary Figure 3SA and B). Specific mice that did not show stimulus–response learning in <30 s or spatial reference memory in <45 s were excluded from further analyses (Table 2). Both the adult and aged KI/Cre and KI/WT mice had a significantly decreased proportion of mice meeting the exclusion criteria compared with the WT/Cre mice. Twenty-four hours after the end of the hidden platform task, included mice were submitted to a single probe for memory retention by removing the platform. The mice were monitored for the percentage of total test time spent in the target quadrant where the platform used to be (percentage of time), the percentage of total distance that the mice swam in

Table 1 Demographic information and cognitive scores of TauΔCasp6-stained human non-cognitively impaired aged individuals

Case	Sex	Age (years)	PMI (h)	Edu (years)	B	Cognition scores						
						Comprehensive		Memory			Perception	
						MMSE	GCS	EP	SE	WO	VSA	PS
1	M	83.40	7.58	15	3	22	−1.20	−1.01	−1.57	−1.31	−0.89	−1.20
2	M	82.97	15.62	16	3	28	−0.62	−0.74	−0.14	−1.13	0.30	−0.87
3	M	90.29	2.83	16	5	27	−0.24	−0.17	0.30	−0.19	−0.27	−1.47
4	M	83.54	5.08	18	4	27	−1.13	−1.39	−1.24	−1.36	0.60	−1.44
5	M	74.29	10.25	19	0	27	0.59	0.61	0.64	0.74	0.74	0.24
6	M	84.16	6.50	15	4	25	−0.68	−0.61	−0.63	−0.84	−0.92	−0.52
7	M	83.73	4.25	16	4	29	0.53	1.30	0.71	−0.29	0.89	−1.27
8	M	92.83	11.03	20	3	26	−0.18	−0.07	0.34	−0.67	−0.14	−0.69
9	M	72.43	7.00	23	2	30	0.69	0.46	0.86	0.40	1.18	1.18
10	F	77.48	3.03	18	3	29	−0.15	0.44	0.56	−1.20	−1.38	−0.26
11	F	91.05	3.33	20	4	28	−0.62	−0.07	0.11	−1.25	−1.36	−1.59
12	F	84.75	5.75	16	3	30	0.71	1.49	0.96	−0.15	0.29	−0.23
13	F	89.41	27.00	19	3	30	0.33	1.07	0.28	0.10	−0.47	−1.00
14	F	79.12	18.22	18	3	30	1.22	1.60	0.90	0.95	1.04	1.28
15	F	92.67	6.28	18	1	27	−0.15	0.44	0.56	−1.20	−1.38	−0.26
16	F	85.48	3.42	20	4	29	0.40	0.95	−0.23	0.32	0.71	−0.66
Mean		84.23	8.57	17.94	2.94	27.63	−0.03	0.27	0.15	−0.44	−0.07	−0.55
S.E.M.		1.54	1.66	0.55	0.34	0.54	0.18	0.23	0.18	0.20	0.23	0.22

the target quadrant where the platform used to be (percentage of distance), and the number of times that the mice crossed directly over where the platform used to be (number of platform crosses).

The KI/Cre, but not the KI/WT nor WT/Cre, mice showed a significant inverse correlation between age and the percentage of time, percentage of distance, and the number of platform crosses (Figure 3a). Averaging the performance of adult (<15 months) and old (≥ 15 months) mice, the old KI/Cre mice specifically displayed a deficit in spatial memory retention (Figure 3b). Although the adult KI/Cre Casp6-expressing mice spent more percentage of time, percentage of distance, and crossed the platform more often in the target quadrant than in the non-target quadrants, the old KI/Cre mice did not. In contrast, both the adult and old KI/WT mice spent more percentage of time, percentage of distance, and crossed the platform more often in the target quadrant than in the non-target quadrants, regardless of age. To assess whether the level of Casp6 expression in the mice brains associate with memory performance, we correlated CA1 Casp6 semi-quantitative immunoreactivity scores (0 = absent, 1 = rare, 2 = frequent, and 3 = abundant immunoreactive neurites; Supplementary Figure S4) with the probe results. The levels of Casp6 immunoreactivity in the CA1, but not in the CA2, inversely correlated with percentage of time ($r = -0.495$; $P = 0.006$), percentage of distance ($r = -0.453$; $P = 0.014$), and number of platform crosses ($r = -0.449$; $P = 0.014$).

Both the adult and old WT/Cre mice performed normally in the stimulus–response learning and spatial reference memory tasks (Supplementary Figures S3A–C), and more mice in the WT/Cre group were included in the memory retention task than the KI/Cre and KI/WT genotypes (Table 2). This indicates that these mice are not visually impaired and are able to learn. Surprisingly, these WT/Cre performed poorly in the memory retention task and did not choose the target quadrant more frequently than the other quadrants. This problem did not exist in the KI/Cre and KI/WT groups as both adult groups performed as expected. Furthermore, when comparing littermate WT/WT to WT/Cre, these performed equally well in the stimulus–response learning and spatial reference memory tasks (Supplementary Figure S3C). However, again the WT/Cre performed poorly in the memory retention task (Figure 3d). The WT/WT mice spent significantly ($P \geq 0.05$) more percentage of time, percentage of distance, or number of platform crossing in the target *versus* the non-target quadrants while the WT/Cre mice did not.

That the adult KI/Cre mice performed well in the memory retention task while the old KI/Cre mice did not suggested that the age-dependent deficit in Casp6-expressing mice is not due to Cre expression. To confirm that the KI/Cre deficit in spatial memory is not an overall problem with Cre expression, we set up the novel object recognition (NOR) test as an alternative measure of memory.

Memory impairment was more robustly detected in old KI/Cre mice (≥ 15 months) with a NOR task. In this task, mice were initially exposed to two identical objects. When one of the familiar objects was replaced with a novel object 2 h after the pre-exposure time to two identical objects, the KI/WT, WT/Cre, and WT/WT mice spent more percentage of distance, percentage of time touching, or crossing over the novel object than the familiar object (Figure 3c; compare familiar with novel), consistent with expected recognition of a novel object. In contrast, the Casp6 KI/Cre mice spent as much time with the novel object as with the familiar object, indicating that they had no recollection of previous interaction with the familiar object. There was a tendency, although not always significant, for all genotypes except KI/Cre to respond less to the familiar object compared with responses made during pre-exposure to that object (Figure 3c). Locomotor ability and anxiety were excluded as possible reasons for the KI/Cre poor performance. Indeed, KI/Cre, KI/WT, WT/Cre, and WT/WT mice did not show any difference, over three consecutive days, in

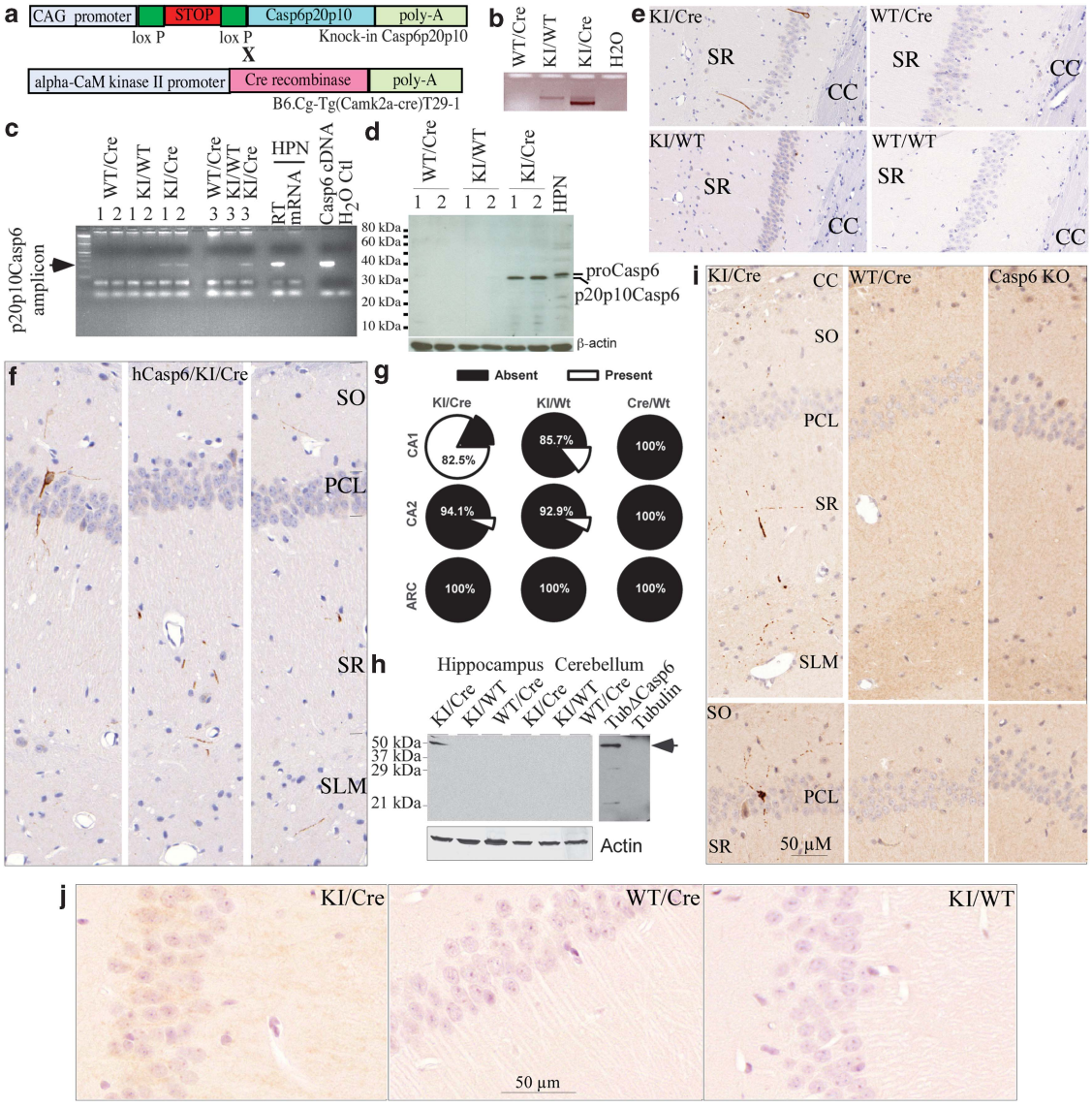

Figure 2 Transgenic model expresses Casp6 in the CA1 of the mouse hippocampus. (**a**) Schematic diagram showing the structure of the transgenic hCasp6 cDNA and CaMKIIa-Cre constructs. (**b**) Ethidium bromide-stained agarose gel showing excision of the Stop sequence in the KI/Cre mouse brain by PCR amplification of the ACL-1 locus (CAG-loxP-STOP-loxP-Casp6p20p10). (**c**) Ethidium bromide-stained agarose gel showing the hCasp6 amplicon from the KI/Cre but not the KI/WT or WT/Cre mice brain. Numbers represent three different cases. HPN, human primary neurons. (**d**) Western blotting of human p20p10Casp6 expression in brain of KI/Cre mice. (**e**) Micrograph of mouse CA1 tissue sections immunopositive for anti-hCasp6 in Casp6 KI/Cre but not in KI/WT, WT/Cre, or WT/WT brains. CC, corpus callosum. Controls to show specificity of the anti-hCasp6 antisera are in Supplementary Figure S2. (**f**) Immunostained hCasp6 distribution in neurites of the SO, PCL, SR, and SLM of the CA1 region. (**g**) Percentage of KI/Cre ($n=17$), KI/WT ($n=14$), WT/Cre ($n=11$) CA1, CA2, or ARC immunopositive for hCasp6. Mice were aged from 2 to 20 months. (**h**) Western blotting showing TubulinΔCasp6 in the KI/Cre hippocampus but not in the cerebellum or in KI/WT and WT/Cre hippocampus and cerebellum. Recombinant full-length tubulin (FL Tub) and Tubulin cleaved by Casp6 (TubΔCasp6) were used as controls. (**i**) Micrograph showing TubulinΔCasp6 immunoreactivity in similar locations of KI/Cre CA1 as observed for hCasp6. Mice hippocampus shown were from 24-month-old KI/Cre and WT/Cre mice, while the Casp6 KO was 12 months old. (**j**) Immunostaining of mouse brains with anti-active Casp6 (Biovision)

percentage of distance, speed, thigmotaxis, or stationary measures when no objects were present in the apparatus (Figure 3d). These activity and anxiety measures remained the same in all genotypes when objects were added to the apparatus (Figure 3e).

Together, the water maze and the NOR test suggest that selective memory impairments related to spatial and EP were observed in aged mice expressing the human form of active Casp6 in the CA1 region of the hippocampus.

Caspase-6 overexpression induces neuronal degeneration and inflammation in the CA1 region of the mouse hippocampus. Cognitive impairment of the Casp6 KI/Cre mouse was accompanied with age-dependent neuritic dystrophy. In younger Casp6 KI/Cre mice aged 4–5 months, hCasp6 was observed mostly in fine neurites of the SO, SR, and SLM (Figure 4a). With aging, beginning at around 8 months of age, hCasp6 was observed occasionally in the soma of CA1 PCL neurons (Figure 4a: examples in 17.4- and

Table 2 Number of mice included in memory retention analysis by water maze

Genotype	Age	No. of mice included	Total no. of mice	% included	Mean rank
KI/Cre	Adult	45	55	81.8	126.63[a]
	Old	24	36	66.7	
KI/WT	Adult	50	62	80.6	126.01[a]
	Old	21	31	67.7	
WT/Cre	Adult	39	41	95.1	103.84
	Old	15	16	93.8	

[a]Kruskal–Wallis test ($\chi^2 = 9.61$, df = 2, $P = 0.008$) revealed that mice with the Casp6 knock-in genotypes had a significantly decreased proportion of mice meeting the criterion for data inclusion compared with the WT/Cre group. Most of the excluded mice (92%) failed the hidden platform criterion

20.1-month PCL). In the oldest mice, occasional Casp6-immunopositive neurons were observed with pycnotic nuclei, and these lacked neuritic Casp6 (24 months PLC) indicating complete degeneration of neurites and ongoing neuronal cell death. In general, Casp6-positive neurites thickened as early as 4–5 months, and these thicker neurites increased in abundance with age. Quantitative assessment indicated that the Casp6-immunopositive neurites were generally larger in old ($n = 4$; 18.62 ± 1.4 months) mice compared with the adult ($n = 3$; 7.6 ± 2.4 months) mice CA1 (Figure 4b). To assess neuronal cell death, NeuN-immunopositive neurons were counted in the entire CA1 area. There was an apparent thinning of the Casp6 KI/Cre PCL in the oldest mice (Figure 4c). Despite a tendency to be lower, the reduction of neuron numbers in the CA1 of KI/Cre mice did not reach statistical significance compared with KI/WT and WT/Cre genotypes (left panel of Figure 4d). However, the number of neurons spanning the PCL of the CA1 was significantly reduced in the old KI/Cre mice (>15 months) compared with old KI/WT and WT/Cre mice (right panel of Figure 4d). Immunostaining for active Casp3 did not reveal significant numbers of immunopositive cells. Only one cell per hippocampal tissue sections was observed in one of the three cases of the KI/Cre mice, and no immunopositive cells were observed in the hippocampus of three individual KI/WT and WT/Cre mice, despite the anti-active Casp3 antibody detecting high numbers of immunopositive cells in brain sections of fetal ischemic tissues (Supplementary Figure 5S). Western blotting analyses of 8–9-month-old mice brains showed a reduction in the levels of synaptophysin and a statistically significant increase in astrocytic glial fibrillary acidic proteins (GFAPs) in the KI/Cre mice compared with WT/Cre mice (Figure 4e). By immunostaining, inflammation was evidenced in KI/Cre mice by an increase of GFAP-immunopositive astrocytes (Figure 4f) and Iba1-immunopositive microglia (Figure 4g) in the SLM of the CA1. This occurred as early as 3 months of age. Bielchowski silver staining also showed higher amounts of silver-stained neurites with a thickened appearance in the KI/Cre CA1 compared with the KI/WT and WT/Cre mice brains (Figure 4h). However, we did not observe significant anti-amyloid immunoreactivity in the form of NP or intraneuronal amyloid accumulation, nor AT-8- or PHF-1-immunopositive tau/tangle pathology, in the Casp6 KI/Cre CA1 region of the hippocampus. This is not entirely surprising as the mouse APP is not particularly amyloidogenic and the mouse Tau is not prone to tangle formation either.

Discussion

Our results show that Casp6 activity in the CA1 of the mouse hippocampus is sufficient to induce spatial and EP impairment. Indeed, spatial retention memory, as assessed by the Morris water maze, indicated impaired cognition in the aged (>15 months) KI/Cre mice but not in the adult KI/Cre (<15 months) or in the adult and aged KI/WT littermates. Although the WT/Cre mice performed well in stimulus–response learning and in spatial reference memory, they did not perform well in the memory retention task of the water maze test. This deficit was age-independent. Others have observed negative effects associated with Cre expression in the developing nervous system and in cardiac tissue;[34,35] however, to our knowledge no reports have indicated a problem in the T29-1 mice. Nevertheless, we do not believe that this problem abrogates our conclusion that the KI/Cre Casp6-expressing mice have an age-dependent spatial memory impairment because when we compare the adult and old KI/Cre, the adult (≤ 15 months) mice show memory retention in the probe test while the old mice show impairment of this function. Furthermore, EP impairment was observed in the aged KI/Cre mice with the NOR assay, while the KI/WT, WT/Cre, and WT/WT littermates had preserved EP. Consequently, we deduce that Casp6 activity in the CA1 of aged mice is causing their decreased performance in EP and spatial memory tasks. By extension, we also deduce that the strong Casp6 activation in sporadic and familial AD[1–3] could be responsible, at least in part, for the cognitive deficits observed in these individuals. NCI individuals do not yet show neuronal loss in the CA1, thus excluding neuronal cell death as the reason for their lower memory performance.[36–39] These results imply that inhibiting Casp6 activation in aged individuals may prevent or significantly delay the progressive loss of cognition and development of dementia in AD.

We observe that memory impairment does not depend on an overall abundance of Casp6 activity at any one time in the CA1 of the mice. Indeed, only a few neurons, at any age, were immunopositively stained with anti-hCasp6 antibodies despite the expected expression of the T29.1 CaMKIIa-Cre in all neurons of the CA1 PCL.[33] However, these results are quite consistent with the observation of a significant decrease in EP and SE performance in human NCI individuals with very low levels of CA1 Casp6 activity (Figure 1d).

This mouse model is the first to show age-dependent Casp6-mediated hippocampal dysfunction in a manner similar to that observed in AD and thus may serve as an excellent model to investigate age-dependent axonal degeneration and memory impairment. That Casp6 expression in the CA1 within 3 weeks of birth does not immediately affect hippocampal function could be explained by increased turnover of the active Casp6 via proteasomal degradation,[40] the presence of ongoing repair mechanisms against Casp6-mediated damage, or the necessity of accruing damage in time before the manifestation of symptoms.

That Casp6-dependent memory impairment occurs in the absence of NP and NFT in our mouse model implies that

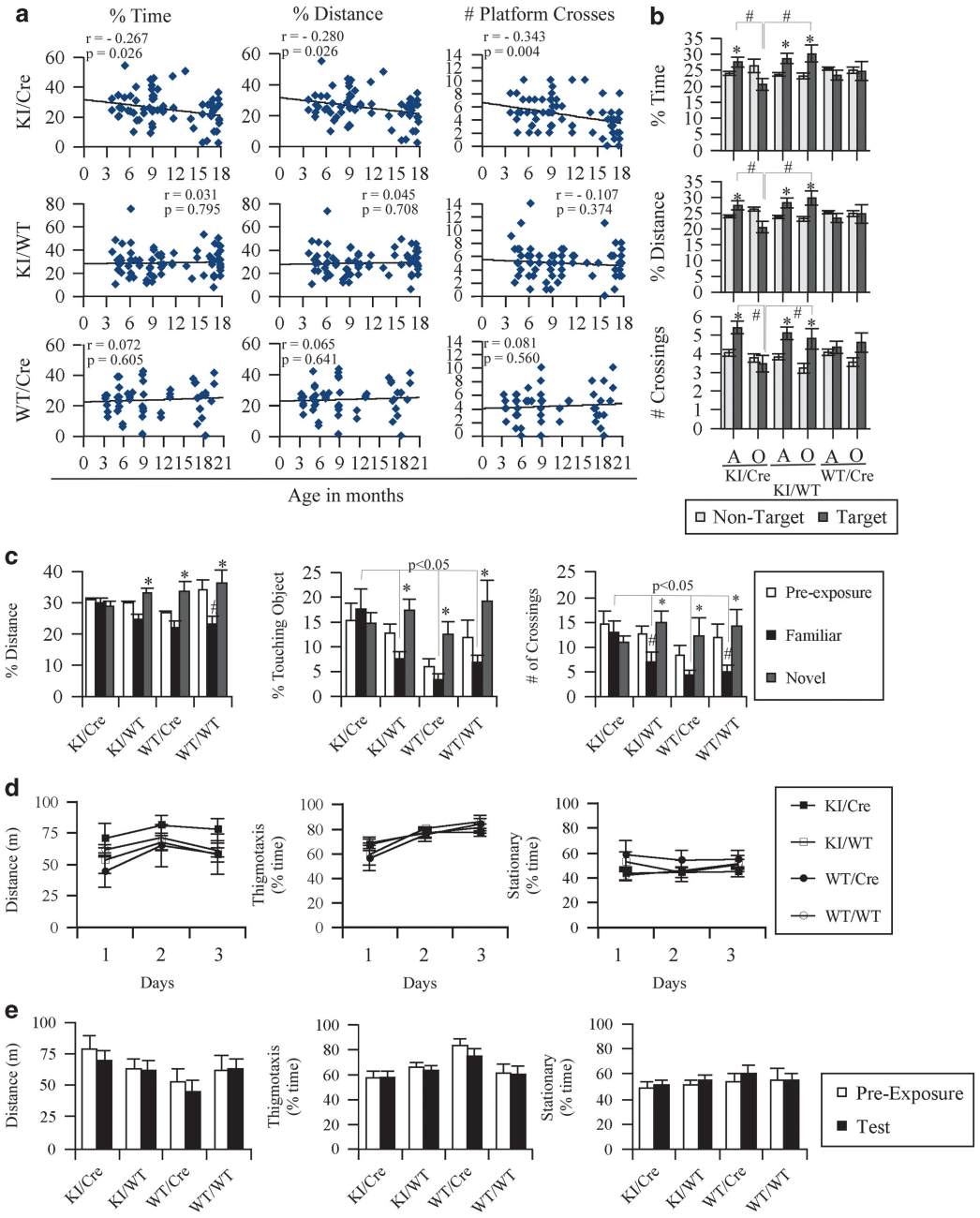

Figure 3 Transgenic mice expressing human active Casp6 in the hippocampal CA1 region undergo age-dependent memory impairment. (**a**) Linear regression of percentage of time, percentage of distance, and the number of platform crosses on probe day (platform removed) *versus* the age of the KI/Cre, KI/WT, and WT/Cre mice. Linear regression *r* and *P* values are indicated within each graph. Supplementary Figures S3A and B shows the results of the initial stimulus–response learning (visible platform) and spatial reference memory (hidden platform) of adult and aged mice groups tested. (**b**) Averaged performance of adult (A ≤ 15 months) and old (O ≥ 15 months) mice in the memory retention probe measured as percentage of time, percentage of distance and number of platform crossings in the target (platform removed) and non-target quadrant. Numbers of mice analyzed per age and genotype are indicated in Table 2. *Compares non-target and target quadrants. #Comparisons are indicated with bars. $^{*,\#}P<0.05$. (**c**) NOR analyses of KI/Cre, KI/WT, WT/Cre, and WT/WT mice showing the percentage of distance, percentage of time touching the object or the number of crossings over the objects in pre-exposure (two similar objects) or with the familiar or novel object. Nine KI/Cre (24.3 ± 0.92 months old; range 20–27 months), 11 KI/WT (24.5 ± 0.89 months old; range 20–27 months), 7 WT/Cre (24.7 ± 1.04 months old; range 21–27 months), and 6 WT/WT (24.7 ± 0.61 months old; range 22–26 months) were tested. Statistical evaluations were done with ANOVA followed by a Tukey *post-hoc* analysis. $^{*}P<0.05$ compared with familiar object and $^{\#}P<0.05$ compared with the pre-exposure assessment. (**d** and **e**) Measures of locomotor activity (distance) and anxiety (thigmotaxis, stationary) in mice used in the NOR test before adding objects in the apparatus (**d**) and after the addition of two identical objects (**e**). No significantly significant difference was observed in any of the genotypes or time in these pre-tests

removal only of Aβ or NFT from AD brain without eliminating Casp6 activity will not be able to stem the progression of the disease. This could explain why removal of Aβ in individuals with mild AD did not delay progression of the disease.[41] Although there is still considerable support for amyloid being a cause of AD,[42] there is also evidence to indicate that Casp6

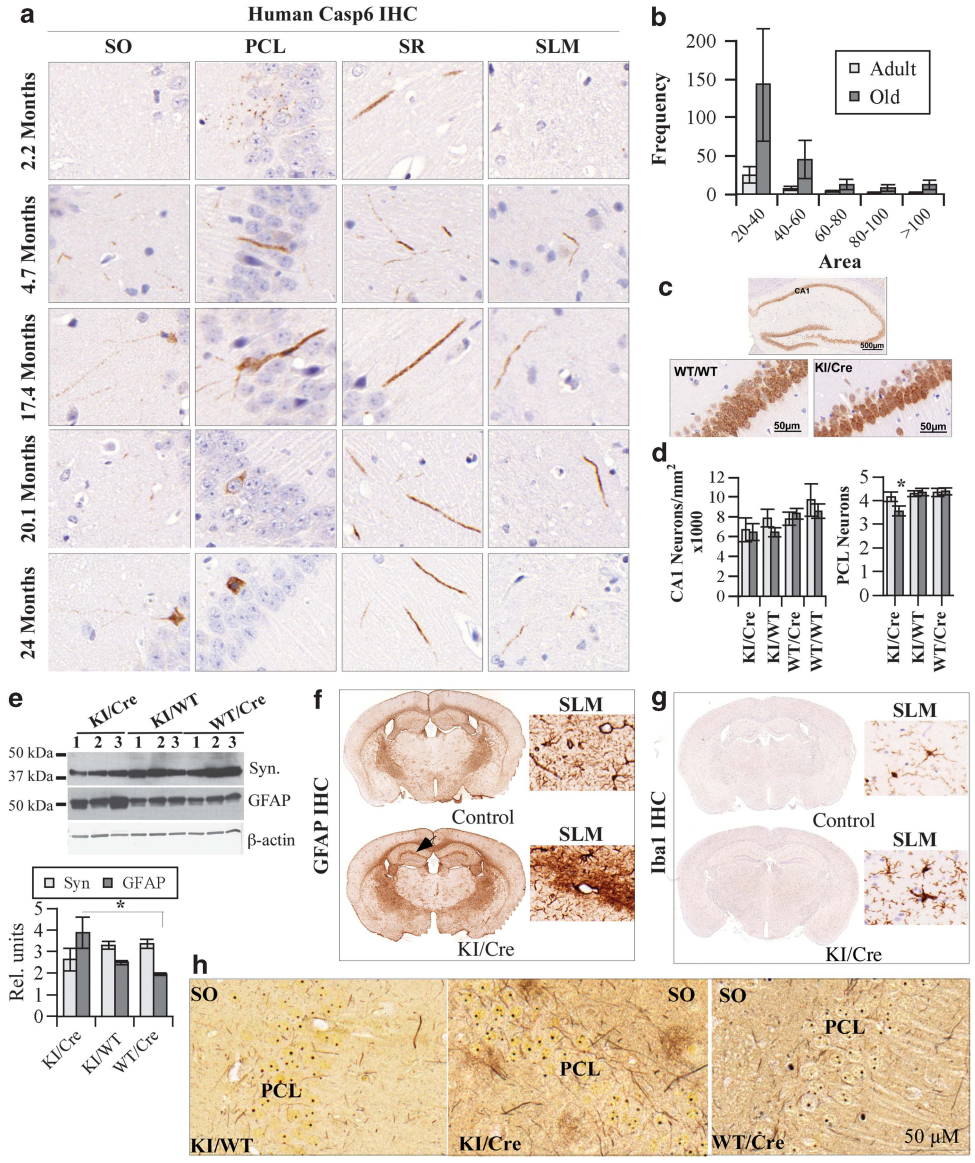

Figure 4 Expression of hCasp6 in CA1 induces neurodegeneration and inflammation. (**a**) Immunohistochemistry (IHC) of hCasp6 in the CA1 SO, PCL, SR, and SLM of Casp6 KI/Cre mice between the ages of 2 and 24 months. Seventeen KI/Cre, 14 KI/T, and 11 WT/Cre mice ranging in age from 2 to 24 months were assessed. (**b**) Frequency of hCasp6-immunopositive areas (separated in bins of 20 pixels) from the CA1 (including SO, PCL, SR, and SLM) in three adult mice and four old mice CA1. The brains were sectioned as coronal sections of 4 μm. The immunopositive areas measured in pixels were from a minimum of three immunostained sections/case and encompassed the entire CA1 from the SLM to the SO of the CA1. Adult indicates $n=3$; 7.5 ± 2.3 months old (range 5–9 months) and old indicates $n=4$ at 18.3 ± 1.8 months old (range 16 to 20 months). (**c**) Representative example of NeuN IHC of the hippocampus, and magnification of the CA1 PCL in a KI/Cre and a WT/WT. (**d**) Left panel: NeuN-immunopositive neurons in the CA1 of adult (<12 months; grey bars) and old (≥ 12 month; dark bars) KI/Cre ($n=4$ adults and 4 old), KI/WT ($n=6$ adults and 3 old), WT/Cre ($n=5$ adults and 5 old), and WT/WT. Bar represents mean ± S.E.M. (**d**) Right panel: Number of NeuN-immunopositive neurons spanning the PCL in KI/Cre ($n=5<$ 15-month adult and $n=3>15$-month old), KI/WT ($n=7$ adults and 3 old), and WT/Cre ($n=7$ adults and 5 old). *$P<0.05$ indicates a difference between the old KI/Cre and old KI/WT or WT/Cre. (**e**) Western blotting of synaptophysin and GFAP in three brains from Casp6 KI/Cre and KI/WT and WT/Cre controls. Bar graph shows densitometric analysis (units of synaptophysin (Syn) or GFAP normalized to actin levels). Asterisk indicates a significant difference between KI/Cre GFAP levels and WT/Cre levels. (**f** and **g**) IHC with GFAP (**f**) or Iba1 (**g**) of control and Casp6 KI/Cre mouse brain. Inset is a magnification of the SLM area. (**h**) Bielchowski silver staining of KI/WT, KI/Cre, and WT/Cre CA1

can be upstream or parallel to Aβ and NFT production: lack of correlation between Aβ and memory performance despite a strong correlation with Casp6 and PHF-1 in aged hippocampi,[6] Casp6-dependent Aβ production in human CNS primary neuron cultures,[15,16] Casp6-dependent, but Aβ-independent, neuritic degeneration in APP-transfected human primary neurons,[14] and caspase activity leading to NFT in mice.[8] Targeting Casp6, in addition to Aβ and NFT, may be required to efficiently prevent AD progression.

In summary, we have shown that hCasp6 expression in mouse CA1 neurons induces neurodegeneration and memory deficits as observed in aged human individuals. These findings infer that blocking Casp6 activity may be essential to prevent cognitive deficits in AD and that eliminating Aβ or

NFT, without preventing Casp6 activity, will be insufficient for the treatment of AD.

Material and Methods

Collection of brain tissues and immunostaining of human brains. Brain tissues were obtained from Religious Orders Study (ROS) subjects.[43] Yearly clinical evaluations by the ROS included a medical history and neurological, cognitive assessments, and clinical diagnoses. Braak staging was performed on autopsied brains by examiners shielded to clinical data. The ROS provided baseline and last valid neuropsychological assessment scores for MMSE, VSA, PS, and EP, SP, and WO, which were converted to *Z* scores (using the mean and S.D. at baseline); a global cognitive score was developed by averaging 19 cognitive function tests. Scores were unveiled once the study was completed. Participants were diagnostically classified by a clinician following the National Institute of Neurological and Communicative Disorders and Stroke and the AD and Related Disorders Association (NINCDS-ADRDA) criteria. NCI referred to persons without dementia or mild cognitive impairment. Sporadic AD brain tissue was obtained from Dr. Catherine Bergeron (University of Toronto, Canada). All human material was obtained with informed consent and under the NIH and CIHR ethical guidelines and regulations. The McGill University Institutional Review Board approved the use of the human tissues in research.

Formalin-fixed, paraffin-embedded 4-μm-thick hippocampal tissue sections were deparaffinized, rehydrated, treated with antigen retrieval buffer (10 mM Tris Base, 1 mM EDTA, 0.05% Tween 20, pH 9) for 20 min at 97 °C in the Pascal Dako Cytomation apparatus, and immunostained using the Dako Autostainer Plus automated slide processor and the EnVision Flex system (Dako, Burlington, ON, Canada). Tissue sections were treated with peroxidase for 5 min, blocked with Serum-Free Protein Block (Dako) for 30 min, submitted to 30 min of neoepitope antisera against active Casp6 (10630: 1/5000) and TauΔCasp6 (10635: 1/25000)[1] diluted in EnVision Flex Antibody Diluent. Immunoreactivity was revealed with mouse/rabbit-HRP secondary antibodies for 30 min and diaminobenzidine (Dako) for 10 min. Slides were counterstained with hematoxylin, dehydrated, mounted in Permount mounting medium (Fisher Scientific, Ottawa, ON, Canada) and digitally scanned with the MIRAX SCAN (Zeiss, Don Mills, ON, Canada). None of the digital images were modified electronically except in the selection of the area for the figures. The Atlas of the Human Brain was used as a reference to identify the CA1 in each tissue section.[44] Image J[45] (http:\\imagej.nih.gov) was used to assess the amount of hCasp6 immunoreactivity in the CA1. Using the scanned tissue sections from the Mirax digital scanner (Don Mills, ON, Canada) 10–15 images were taken at $\times$ 20 from each of the 16 NCI cases. In Image J, max. entropy threshold method and Lab color space was applied. The color adjustment tool was used to remove the background and convert the immunoreactivity to black. Particles of all sizes were analyzed. An arithmetic mean was calculated from the count of the five most involved fields. The results were expressed as CA1 TauΔCasp6 counts/mm^2. Correlations between cognitive scores and CA1 TauΔCasp6 pathology were assessed with the non-parametric Spearman's rank test (two-tailed, $P<0.05$ was taken as statistical significance).

Generating the transgenic mouse model expressing a self-activating form of Caspase-6. All animal procedures followed the Canadian Council on Animal Care guidelines and were approved by the McGill Animal care committees. Mice were bred and aged in the Goodman Cancer Research Centre Mouse Transgenic Facility at McGill University. The conditional expression mouse line expressing hCasp6 was made with Quick knock-in technology (Genoway, Lyon, France). The hCasp6 cDNA lacks its pro-domain (p20p10Casp6) to promote self-activation upon expression in mammalian cells.[22] The p20p10Casp6 cDNA was placed under the control of the ubiquitous and strong CAG promoter (CMV immediate early enhancer/chicken β-actin promoter fusion). A LoxP flanked STOP cassette was inserted between the promoter and the transgene to allow regulation of expression by Cre excision of the STOP sequence. The transgene was knocked-in in the hypoxanthine-guanine phosphoribosyl transferase (HPRT) locus of chromosome X thereby avoiding problems caused by the non-targeted insertion of the transgene throughout the genome. The KI was transfected in 129/Ola cells, and these cells were injected into C57Bl6 mice. The mice have been crossed with the Calmodulin kinase II (CaMKII)-regulated Cre expression mouse (T29.1).[33] The 29.1 (in C57Bl/6 background) was reported to exclusively express Cre in the CA1 pyramidal neurons of the hippocampus and in the scattered neurons of the forebrain approximately at 2–3 weeks after birth.[33] All mice are viable and reproduce well. Same sex littermates were group-housed (2–4 animals per cage) in standard macrolon cages ($40 \times 25 \times 20\,cm^3$) under a 12-h light/dark schedule in controlled environmental conditions of humidity (60%) and temperature (21 °C) with food and water supplied *ad libitum*. Only male mice were used in the analysis.

RT-PCR of hCasp6 p20p10cDNA from the mice brains. Total RNA was extracted from brain tissue with Trizol (Invitrogen, Burlington, ON, Canada). The first-strand cDNA synthesis reaction was performed with avian myeloblastosis virus reverse transcriptase, as recommended (Roche Applied Sciences, Montreal, QC, Canada). PCR amplification of human p20p10Casp6 was done with primers 5′-CGATGTGCCAGTCATTCCTT-3′ and 5′-CTCTAAGGAGGAGCCATATTTTC-3′ and Taq DNA polymerase (U.S. Biochemical Corp., Santa Clara, CA, USA) under the standard conditions. The PCR yielded the expected 229-bp amplicon. Human primary neuron RNA was used as a positive control for hCasp6. These neurons were obtained as previously described[15] from fetal human brain acquired under ethical consent according to the guidelines and regulations of the NIH and CIHR.

Western blotting analysis of the mice brains. Mice were killed with CO_2, and the brains were immediately removed. Hippocampus cortex and cerebellum were dissected and frozen on a dry ice slab immediately. Tissues were kept at -80 °C until use. Brain cortex, hippocampus, or primary human neuron proteins were extracted by mechanical homogenization with a Kinematica Polytron in cell lysis buffer (CLB; 50 mM HEPES (2-[4-(2-hydroxyethyl)piperazin-1-yl]ethanesulfonic acid), 0.1 mM EDTA, 1 mM dithiothreitol, 0.1% CHAPS (3-[(3-cholamidopropyl) dimethylammonio]-1-propanesulfonate)) supplemented with protease inhibitors (38 μg/ml AEBSF (4-(2-aminoethyl) benzenesulfonyl fluoride hydrochloride), 0.5 μg/μl pepstatin A, 1 μg/ml TLCK, 0.5 μg/ml leupeptin). Extracts were centrifuged at $12\,000 \times g$ for 5 min, and the pellet was resuspended in $1\times$ radioimmunoprecipitation assay buffer ($1\times$ RIPA—50 mM Tris-HCl pH 8.0, 150 mM NaCl, 1% NP-40, 0.5% sodium deoxycholate, 0.1% SDS). Protein concentration was quantified by the colorimetric Bradford assay (Bio-Rad Laboratories, Mississauga, ON, Canada). One hundred micrograms each of CLB supernatant protein and RIPA-solubilized protein was pooled, precipitated in $4\times$ volume of cold acetone containing 0.07% β-mercaptoethanol, and resuspended in 30 μl of $1\times$ SDS Laemmli buffer. Western blots were probed with 1 : 500 Neomarker Ab-4 rabbit Caspase-6 antibody (Neomarkers) or mouse β-actin primary antibody (1 : 5000) (Sigma, St. Louis, MO, USA), followed by HRP-linked secondary antibody detection (1 : 5000) (GE Amersham, Montreal, QC, Canada) with ECLPlus western blotting detection system (GE Amersham). For TubulinΔCasp6, brains were extracted in CLB, separated on 10% polyacrylamide gel electrophoresis (PAGE), and immunoblotted with a 1/1000 dilution of neoepitope antisera against TubulinΔCasp6.[7] Full-length tubulin was purchased from Cytoskeleton Inc. (Denver, CO, USA) and incubated with or without recombinant active Casp6 for the negative and positive control. For synaptophysin and GFAP detection, brains were extracted in $1\times$ RIPA and the extract sonicated for 30 s. Proteins were separated on 10% PAGE and immunoblotted with mouse anti-synaptophysin (Sigma) at 1/500 dilution and rabbit anti- GFAP at 1/3000. Densitometric analyses of the protein bands was done by scanning the X-ray film on the ChemiGenius apparatus (Syngene, Frederik, MD, USA) using a lower light setting in transmission mode, and bands were analyzed using Image J.

Excision of the STOP sequence with Cre recombinase. Genomic DNA was extracted with Trizol according to the manufacturer's protocol. Twenty nanograms of genomic DNA was used as template to amplify the recombined or Cre-excised recombined HPRT locus using primers designed by Genoway: Forward 5′-TGCTTCAGTCCCATGTTTGGCAAGG-3′ (GX5889) and Reverse 5′-AAATCTGTG CGGAGCCGAAATCTGG-3′ (GX2752) and standard protocols. The recombined HPRT locus and Cre-excised recombined HPRT locus generate a 4195 and 2812 bp amplicon, respectively.

Immunohistological and Bielchowski staining of mice brains. Mice were initially perfused with saline and then 4% paraformaldehyde prepared fresh. Brains were removed and placed in 10% neutral-buffered formalin (Fisher Scientific) for 24 h and changed to 70% ethanol for 24 h. Fixed brains were paraffin embedded, and sections were cut at 6 μm for immunohistochemistry at the IRIC histology core facility (University de Montreal, Montreal, Canada). Immunostaining was conducted as described above for human brain tissue sections. Epitopes were demasked in EDTA pH 9 buffer. The following antibodies were used in mouse brains: rabbit anti-hCasp6 LSB477 (1/5000, Lifespan Bioscience, Seattle, WA, USA),

rabbit anti-TubulinΔCasp6 (1/6000 dilution[7]), rabbit anti-GFAP (1/8000, Dako), rabbit monoclonal anti-Iba1 (1/2000, Wako, Richmond, VA, USA), mouse anti-NeuN (1/2000, Millipore, Etobicoke, ON, Canada), and Biovision anti-active Casp6 (1/100, Mountain View, CA, USA). The TubulinΔCasp6 antiserum was raised in rabbit as a neo-epitope antiserum against the human tubulin sequence EEVEGD[438] that was conjugated to keyhole limpet hemocyanin via a cysteine at the N-terminus of the peptide sequence.[7] In western blots, this antiserum detects only the recombinant alpha-tubulin cleaved by Casp6 and not full-length alpha-tubulin[7] and endogenously expressed alpha-tubulinΔCasp6 in Casp6-transfected cells.[22] In immunohistochemical analyses, the TauΔCasp6 antiserum detects neurons in AD brains tissue but not in age-matched controls and in younger brains.[7] Immunohistochemistry with TubulinΔCasp6 was tested in 10 KI/Cre mice hippocampus aged 7–24 months, seven age-matched WT/Cre and six age-matched KI/WT, some of these were littermates. The TauΔCasp6 antiserum was also raised in rabbit against human Tau sequence KSPVVSGD[402].[1]

Image J was used to assess the size of each area immunopositive for hCasp6 on three immunostained sections for each mouse brain. The brains were sectioned as coronal sections of 4 μm. The immunopositive areas measured in pixels were from a minimum of three immunostained sections/case and encompassed the entire CA1 from the SLM to the SO of the CA1. In Figure 4b, adult indicates $n = 3$; 7.5 ± 2.3 months old (range 5–9 months) and old indicates $n = 4$ at 18.3 ± 1.8 months old (range 16–20 months). Bins were set at 20 pixels. The Bielchowski staining was done with a protocol used in the McGill Department of Anatomic pathology at the IRIC core histology facility. Briefly, slides were deparaffinized, hydrated, microwaved in 20% silver nitrate for 2 min, followed by a similar treatment with ammonia hydroxide-cleared silver nitrate solution, and developed with a 10% formaldehyde, 0.5% citric acid, and one drop of nitric acid solution in water. Development was allowed until golden brown and stopped in distilled water. Each slide was done blinded to the mouse genotype.

Immunohistological assessments of hCasp6 in the mice brains. From three consecutive sections scanned on the Mirax digital scanner, we identified the presence or absence of hCasp6 immunoreactivity in the CA1 and CA2 region of the hippocampus, as well as, in a hypothalamic structure, the ARC. To determine how effective the mouse model was at generating hCasp6 expression in the appropriate genotypes and brain region, a Chi-square analysis was performed on the proportion of mice observed with the presence or absence of Casp6 immunoreactivity in each of the regions. Finally, a semi-quantitatively score was generated by assigning 0 (absent), 1 (rare), 2 (frequent), and 3 (abundant) to each of the three brain sections. These numbers were added, possible scores 0–3, and used for partial correlations controlling for genotype with water maze probe scores.

Morris water maze task. The Morris water maze test was performed mostly as described.[46] The experimenter was blinded to the mouse genotype. Littermates were used to perform the water maze. Water maze was conducted on five separate groups of mice: group I (4–6-month-old males) consisted of 13 KI/Cre, 16 KI/WT, and 11 WT/Cre, group II (8–11-month-old males) consisted of 14 KI/Cre, 12 KI/WT, and 10 WT/Cre, group III (10–18-month-old males) consisted of 10 KI/Cre, 7 KI/WT, and 10 WT/Cre, group IV (16–17-month-old males) consisted of 14 KI/Cre, 18 KI/WT, and 6 WT/Cre, group V (3–19-month-old females) consisted of 40 KI/Cre, 40 KI/WT, and 20 WT/Cre mice. Each male group was tested together over the 9-day period. The female group V was split in two batches tested on the same day for 9 consecutive days.

The water was made opaque with powdered Tempera white no.46 gouache obtained at local art stores. A cued task was performed using a demarked platform that was above the water and varied in location for three trials a day on 3 consecutive days (maximum of 60 s/trial). Acquisition for the spatial task was performed with a hidden platform submerged just below the opaque water and remained in a static location for three trials a day on 5 consecutive days (maximum of 90 s/trial). The latency to reach the platform was recorded with the HSV2100 automated tracking system (HSV Image, Hampton, UK). Twenty-four hours after the last spatial task trial, a single probe trial assessed memory retention for the hidden platform location during which the platform was removed. To be included in the memory retention analyses, mice had to reach the visible platform in < 30 s and perform the spatial task in < 45 s. The percentage of time, percentage of distance, and number of platform crossings in the quadrant previously containing the platform was measured with the HVS system. Statistical analyses for the single probe was done with a 3 (genotypes: KI/Cre, KI/WT, WT/Cre) $\times$ 2 ages (adult and old) $\times$ 2 quadrant (target and non-target) ANOVA on percentage of time, percentage of distance, and number of platform crossings. Pearson's correlations (two-tailed, $P < 0.05$) were used to assess the relationship between spatial memory at probe with the age separately for each of the genotypes and Casp6 scores controlling for genotype.

NOR task. Using the empty white circular water maze pool and the HVS 2100 automated tracking system, mice were allowed to explore the apparatus for three daily 10-min sessions. Twenty-four hours after the last activity session, the mice were allowed to explore two identical objects (pre-exposure), and after 2 h they were presented with the familiar and a novel object. The total distance travelled (m), speed (m/sec), and time spent (s) stationary or engaged in thigmotaxis was recorded. Additionally, distance traveled (percentage of of total) and time spent touching (percentage of of 10 min), and the number of times crossing over a given object was recorded. Behavioral responses to objects were assessed with a 4 (genotypes) $\times$ 3 (pre-exposure, familiar object, novel object) ANOVA performed on distance travelled around (percentage of of total), time spent touching (percentage of of 10 min), and frequency of crossing over a given object. For the pre-exposure analyses, measures were averaged across the two similar objects making the data comparable to novel and familiar object behavioral responses. NOR was conducted blinded to the genotype and littermates from each genotype were tested together. Nine KI/Cre (24.3 ± 0.92 months old; range 20–27 months), 11 KI/WT (24.5 ± 0.89 months old; range 20–27 months), 7 WT/Cre (24.7 ± 1.04 months old; range 21–27 months), and 6 WT/WT (24.7 ± 0.61 months old; range 22–26 months) mice were tested in three independent experiments. Each experiment was conducted with equivalent numbers of mice per genotype.

Acknowledgements. This work was supported by the Canadian Foundation of Innovation, Canadian Institutes of Health Research (CIHR) MOP-243413-BCA-CGAG-45097 to ALB, CIHR MOP-84275 to EH and, in part, by the National Institute of Aging P30AG10161 and R01AG15819 to DAB. We thank Dr. Ann Brasey and Dr. Jenna Ross for the immunostaining, Dr. Olivier Maes for genomic characterization of the transgene in the initial mice, Andrea Lee for the western blotting of synaptophysin, Andrea Hebert-Losier for NeuN counts and densitometry, Dr. Xinkang Tong and Panayiota Papadopoulos for their contribution to teaching the Morris Water Maze technique, and Janice Penney for help with setting up breeding and animal care.

1. Guo H, Albrecht S, Bourdeau M, Petzke T, Bergeron C, LeBlanc AC. Active Caspase-6 and Caspase-6 cleaved Tau in neuropil threads, neuritic plaques and neurofibrillary tangles of Alzheimer's disease. *Am J Pathol* 2004; **165**: 523–531.
2. Albrecht S, Bogdanovic N, Ghetti B, Winblad B, LeBlanc AC. Caspase-6 activation in familial Alzheimer disease brains carrying amyloid precursor protein or presenilin I or presenilin II mutations. *J Neuropathol Exp Neurol* 2009; **68**: 1282–1293.
3. Albrecht S, Bourdeau M, Bennett D, Mufson EJ, Bhattacharjee M, LeBlanc AC. Activation of caspase-6 in aging and mild cognitive impairment. *Am J Pathol* 2007; **170**: 1200–1209.
4. Braak H, Braak E. Staging of Alzheimer's disease-related neurofibrillary changes. *Neurobiol Aging* 1995; **16**: 271–278, discussion 278–284.
5. Braak H, Alafuzoff I, Arzberger T, Kretzschmar H, Del Tredici K. Staging of Alzheimer disease-associated neurofibrillary pathology using paraffin sections and immunocytochemistry. *Acta Neuropathol (Berl)* 2006; **112**: 389–404.
6. Ramcharitar J, Afonso VM, Albrecht S, Bennett DA, LeBlanc AC. Caspase-6 activity predicts lower episodic memory ability in aged individuals. *Neurobiol Aging* 2013; **34**: 1815–1824.
7. Klaiman G, Petzke TL, Hammond J, LeBlanc AC. Targets of caspase-6 activity in human neurons and Alzheimer disease. *Mol Cell Proteomics* 2008; **7**: 1541–1555.
8. de Calignon A, Fox LM, Pitstick R, Carlson GA, Bacskai BJ, Spires-Jones TL *et al.* Caspase activation precedes and leads to tangles. *Nature* 2010; **464**: 1201–1204.
9. Nikolaev A, McLaughlin T, O'Leary DD, Tessier-Lavigne M. APP binds DR6 to trigger axon pruning and neuron death *via* distinct caspases. *Nature* 2009; **457**: 981–989.
10. Simon DJ, Weimer RM, McLaughlin T, Kallop D, Stanger K, Yang J *et al.* A caspase cascade regulating developmental axon degeneration. *J Neurosci* 2012; **32**: 17540–17553.
11. Cusack CL, Swahari V, Hampton Henley W, Michael Ramsey J, Deshmukh M. Distinct pathways mediate axon degeneration during apoptosis and axon-specific pruning. *Nat Commun* 2013; **4**: 1876.
12. Park KJ, Grosso CA, Aubert I, Kaplan DR, Miller FD. p75NTR-dependent, myelin-mediated axonal degeneration regulates neural connectivity in the adult brain. *Nat Neurosci* 2010; **13**: 559–566.

13. Uribe V, Wong BK, Graham RK, Cusack CL, Skotte NH, Pouladi MA *et al.* Rescue from excitotoxicity and axonal degeneration accompanied by age-dependent behavioral and neuroanatomical alterations in caspase-6-deficient mice. *Hum Mol Gen* 2012; **21**: 1954–1967.
14. Sivananthan S, Lee A, Goodyer CG, LeBlanc AC. Familial amyloid precursor protein mutants cause caspase-6-dependent but amyloid β-peptide-independent neuronal degeneration in primary human neuron cultures. *Cell Death Dis* 2010; **1**: e100.
15. LeBlanc A. Increased production of 4 kDa amyloid beta peptide in serum deprived human primary neuron cultures: possible involvement of apoptosis. *J Neurosci* 1995; **15**: 7837–7846.
16. LeBlanc AC, Liu H, Goodyer C, Bergeron C, Hammond J. Caspase-6 role in apoptosis of human neurons, amyloidogenesis and Alzheimer's disease. *J Biol Chem* 1999; **274**: 23426–23436.
17. Pellegrini L, Passer B, Tabaton M, Ganjei K, D'Adamio L. Alternative, non-secretase processing of Alzheimer's ß-amyloid precursor protein during apoptosis by caspase-6 and -8. *J Biol Chem* 1999; **274**: 21011–21016.
18. Gervais F, Xu D, Robertson G, Vaillancourt J, Zhu Y, Huang J *et al.* Involvement of caspases in proteolytic cleavage of Alzheimer's ß-amyloid precursor protein and amyloidogenic ß-peptide formation. *Cell* 1999; **97**: 395–406.
19. Tesco G, Koh YH, Kang EL, Cameron AN, Das S, Sena-Esteves M *et al.* Depletion of GGA3 stabilizes BACE and enhances beta-secretase activity. *Neuron* 2007; **54**: 721–737.
20. Tesco G, Koh YH, Tanzi RE. Caspase activation increases beta-amyloid generation independently of caspase cleavage of the beta-amyloid precursor protein (APP). *J Biol Chem* 2003; **278**: 46074–46080.
21. Halawani D, Tessier S, Anzellotti D, Bennett DA, Latterich M, LeBlanc AC. Identification of Caspase-6-mediated processing of the valosin containing protein (p97) in Alzheimer's disease: a novel link to dysfunction in ubiquitin proteasome system-mediated protein degradation. *J Neurosci* 2010; **30**: 6132–6142.
22. Klaiman G, Champagne N, LeBlanc AC. Self-activation of Caspase-6 *in vitro* and *in vivo*: Caspase-6 activation does not induce cell death in HEK293T cells. *Biochim Biophys Acta* 2009; **1793**: 592–601.
23. Gray DC, Mahrus S, Wells JA. Activation of specific apoptotic caspases with an engineered small-molecule-activated protease. *Cell* 2010; **142**: 637–646.
24. Allsopp TE, McLuckie J, Kerr LE, Macleod M, Sharkey J, Kelly JS. Caspase 6 activity initiates caspase 3 activation in cerebellar granule cell apoptosis. *Cell Death Differ* 2000; **7**: 984–993.
25. Leong SM, Tan BX, Bte Ahmad B, Yan T, Chee LY, Ang ST *et al.* Mutant nucleophosmin deregulates cell death and myeloid differentiation through excessive caspase-6 and -8 inhibition. *Blood* 2010; **116**: 3286–3296.
26. Rust C, Wild N, Bernt C, Vennegeerts T, Wimmer R, Beuers U. Bile acid-induced apoptosis in hepatocytes is caspase-6-dependent. *J Biol Chem* 2009; **284**: 2908–2916.
27. Srinivasula SM, Fernandes-Alnemri T, Zangrilli J, Robertson N, Armstrong RC, Wang L *et al.* The Ced-3/interleukin 1beta converting enzyme-like homolog Mch6 and the lamin-cleaving enzyme Mch2alpha are substrates for the apoptotic mediator CPP32. *J Biol Chem* 1996; **271**: 27099–27106.
28. Orth K, Chinnaiyan AM, Garg M, Froelich CJ, Dixit VM. The CED-3/ICE-like protease Mch2 is activated during apoptosis and cleaves the death substrate lamin A. *J Biol Chem* 1996; **271**: 16443–16446.
29. Takahashi A, Alnemri ES, Lazebnik YA, Fernandes-Alnemri T, Litwack G, Moir RD *et al.* Cleavage of lamin A by Mch2 alpha but not CPP32: multiple interleukin 1 beta-converting enzyme-related proteases with distinct substrate recognition properties are active in apoptosis. *Proc Natl Acad Sci USA* 1996; **93**: 8395–8400.
30. Slee EA, Adrain C, Martin SJ. Executioner caspase-3, -6, and -7 perform distinct, non-redundant roles during the demolition phase of apoptosis. *J Biol Chem* 2001; **276**: 7320–7326.
31. Ruchaud S, Korfali N, Villa P, Kottke TJ, Dingwall C, Kaufmann SH *et al.* Caspase-6 gene disruption reveals a requirement for lamin A cleavage in apoptotic chromatin condensation. *EMBO J* 2002; **21**: 1967–1977.
32. Stoub TR, De Toledo-Morrell L, Stebbins GT, Leurgans S, Bennett DA, Shah RC. Hippocampal disconnection contributes to memory dysfunction in individuals at risk for Alzheimer's disease. *Proc Natl Acad Sci USA* 2006; **103**: 10041–10045.
33. Tsien JZ, Chen DF, Gerber D, Tom C, Mercer EH, Anderson DJ *et al.* Subregion- and cell type-restricted gene knockout in mouse brain. *Cell* 1996; **87**: 1317–1326.
34. Buerger A, Rozhitskaya O, Sherwood MC, Dorfman AL, Bisping E, Abel ED *et al.* Dilated cardiomyopathy resulting from high-level myocardial expression of Cre-recombinase. *J Card Fail* 2006; **12**: 392–398.
35. Forni PE, Scuoppo C, Imayoshi I, Taulli R, Dastru W, Sala V *et al.* High levels of Cre expression in neuronal progenitors cause defects in brain development leading to microencephaly and hydrocephaly. *J Neurosci* 2006; **26**: 9593–9602.
36. West MJ. Regionally specific loss of neurons in the aging human hippocampus. *Neurobiol Aging* 1993; **14**: 287–293.
37. West MJ, Coleman PD, Flood DG, Troncoso JC. Differences in the pattern of hippocampal neuronal loss in normal ageing and Alzheimer's disease. *Lancet* 1994; **344**: 769–772.
38. Gomez-Isla T, Price J, McKeel D, Morris J, Growdon J, Hyman B. Profound loss of layer II entorhinal cortex neurons occurs in very mild Alzheimer's disease. *J Neurosci* 1997; **16**: 4491–4500.
39. Price JL, Ko AI, Wade MJ, Tsou SK, McKeel DW, Morris JC. Neuron number in the entorhinal cortex and CA1 in preclinical Alzheimer disease. *Arch Neurol* 2001; **58**: 1395–1402.
40. Tounekti O, Zhang Y, Klaiman G, Goodyer CG, LeBlanc A. Proteasomal degradation of caspase-6 in 17beta-estradiol-treated neurons. *J Neurochem* 2004; **89**: 561–568.
41. Holmes C, Boche D, Wilkinson D, Yadegarfar G, Hopkins V, Bayer A *et al.* Long-term effects of Abeta42 immunisation in Alzheimer's disease: follow-up of a randomised, placebo-controlled phase I trial. *Lancet* 2008; **372**: 216–223.
42. Karran E, Mercken M, De Strooper B. The amyloid cascade hypothesis for Alzheimer's disease: an appraisal for the development of therapeutics. *Nat Rev Drug Discov* 2011; **10**: 698–712.
43. Bennett DA, Schneider JA, Buchman AS, Barnes LL, Boyle PA, Wilson RS. Overview and findings from the rush memory and aging project. *Curr Alzheimer Res* 2012; **9**: 646–663.
44. Mai JK, Paxinos G, Voss T. *Atlas of the Human Brain*. 3rd edn Elsevier: Amsterdam, the Netherlands, 2008.
45. Schneider CA, Rasband WS, Eliceiri KW. NIH Image to ImageJ: 25 years of image analysis. *Nat Methods* 2012; **9**: 671–675.
46. Nicolakakis N, Aboulkassim T, Aliaga A, Tong XK, Rosa-Neto P, Hamel E. Intact memory in TGF-beta1 transgenic mice featuring chronic cerebrovascular deficit: recovery with pioglitazone. *J Cereb Blood Flow Metab* 2011; **31**: 200–211.

Supplementary Information accompanies this paper on Cell Death and Differentiation website (http://www.nature.com/cdd)